TWENTY FIRST EUROPEAN ROTORCRAFT FORUM

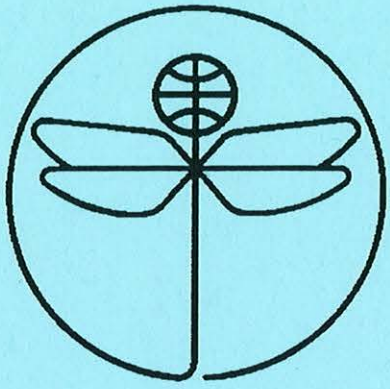

Paper No VI.9

HELICOPTER INDIVIDUAL-BLADE-CONTROL: PROMISING TECHNOLOGY FOR THE FUTURE HELICOPTER

BY

Norman D. Ham

M.I.T
Cambridge,MA
U.S.A

August 30 - September 1, 1995
SAINT - PETERSBURG, RUSSIA

Paper nr.: VI.9

Helicopter Individual - Blade - Control: Promising Technology for the Future Helicopter.

N.D. Ham

TWENTY FIRST EUROPEAN ROTORCRAFT FORUM
August 30 - September 1, 1995 Saint-Petersburg, Russia

HELICOPTER INDIVIDUAL-BLADE-CONTROL: PROMISING TECHNOLOGY FOR THE FUTURE HELICOPTER

Professor Norman D. Ham
Massachusetts Institute of Technology

ABSTRACT

The history, principles, and applications of helicopter individual-blade-control are described, with particular reference to MIT research in the area from 1977 to present.

The emphasis is on wind tunnel and flight testing of full-size rotors since 1986. IBC applications considered are flight stabilization, gust alleviation, lag damping augmentation and vibration alleviation.

Future work on IBC will be briefly outlined.

1. INTRODUCTION

The concept of Individual-Blade-Control (IBC) embodies the control of broadband electrohydraulic actuators attached to each blade, using signals from sensors mounted on the blades to supply appropriate control commands to the actuators. Note that IBC involves not only control of each blade independently, but also a feedback loop for each blade in the rotating frame. In this manner it becomes possible to reduce the severe effects of atmospheric turbulence, retreating blade stall, blade-vortex interaction, blade-fuselage interference, and blade and rotor instabilities, while providing improved performance and flying qualities [1-10].

It is evident that the IBC system will be most effective if it is comprised of several sub-systems, each controlling a specific mode, e.g., the blade flapping mode, the first blade flatwise bending mode, and the first blade lag mode [2]. Each sub-system operates in its appropriate frequency band.

Consider the modal equation of motion

$$m\ddot{x} + c\dot{x} + kx = F(t) + \Delta F \tag{1}$$

where the modal control force ΔF is

$$\Delta F = -K_A c\ddot{x} - K_R c\dot{x} - K_P kx \tag{2}$$

Then substituting (2) into (1)

$$(1+K_A)m\ddot{x} + (1+K_R)c\dot{x} + (1+K_P)kx = F(t)$$

For the case $K_A = K_R = K_P = K$

$$m\ddot{x} + c\dot{x} + kx = [1/(1+K)]\, F(t)$$

and the modal response is attenuated by the factor $1/(1+K)$ while the modal damping and natural frequency are unchanged.

For modal damping augmentation, only the rate feedback $\Delta F = -K_R c\dot{x}$ is required.

The configuration considered in [1-7] employs an individual actuator and multiple feedback loops to control each blade. These actuators and feedback loops rotate with the blades and, therefore, a conventional swash plate is not required. However, some applications of individual-blade-control can be achieved by placing the actuators in the non-rotating system and controlling the blades through a conventional swash plate as described in Section 6 and in [8].

The following sections describe the design of a system controlling blade flapping, bending, and lag dynamics, and related testing of the system on a model rotor in the wind tunnel. The control inputs considered are blade pitch changes proportional to blade flapping and bending acceleration, velocity, and displacement, and lag velocity.

Also presented are preliminary flight test results from a Black Hawk helicopter having two flatwise-oriented accelerometers mounted on one blade. These open-loop results are to be used in the design of an active control system for rotor gust alleviation and attitude stabilization.

2. DETERMINATION OF BLADE MODAL RESPONSE

From Figures 1 and [3], the blade flatwise acceleration at station r due to response of the first two flatwise modes is

$$a(r) = (r-e)\,\ddot{\beta}(t) + r\Omega^2\beta(t) + \eta(r)\ddot{q}(t) + r\Omega^2\eta'(r)q(t)$$

Then, for accelerometers mounted at r_1, r_2, r_3, and r_4

$$\begin{bmatrix} a_1 \\ a_2 \\ a_3 \\ a_4 \end{bmatrix} = \begin{bmatrix} (r_1-e) & r_1\Omega^2 & \eta(r_1) & r_1\Omega^2\eta'(r_1) \\ (r_2-e) & r_2\Omega^2 & \eta(r_2) & r_2\Omega^2\eta'(r_2) \\ (r_3-e) & r_3\Omega^2 & \eta(r_3) & r_3\Omega^2\eta'(r_3) \\ (r_4-e) & r_4\Omega^2 & \eta(r_4) & r_4\Omega^2\eta'(r_4) \end{bmatrix} \cdot \begin{bmatrix} \ddot{\beta} \\ \beta \\ \ddot{q} \\ q \end{bmatrix}$$

In matrix notation, $A = M \cdot R$
Then the flatwise modal responses are given by

$$R = M^{-1} \cdot A$$

Note that the elements of M^{-1} are dependent only upon blade spanwise station, rotor rotation speed, and bending mode shape, i.e., they are independent of flight condition.

Similarly, the blade lag acceleration at station r due to response ζ of the first lag mode can be shown to be [6]

$$a_L = (r - e_L)\ddot{\zeta} + e_L\Omega^2\zeta$$

where e_L is the spanwise location of the lag hinge. Then for accelerometers mounted at r_1 and r_2

$$\begin{bmatrix} a_{L_1} \\ a_{L_2} \end{bmatrix} = \begin{bmatrix} (r_1-e_L) & e_L\Omega^2 \\ (r_2-e_L) & e_L\Omega^2 \end{bmatrix} \cdot \begin{bmatrix} \ddot{\zeta} \\ \zeta \end{bmatrix}$$

In matrix notation $A_L = M_L \cdot R_L$

The lag modal responses are given by

$$R_L = M_L^{-1} \cdot A_L$$

Since the elements of M^{-1} and M_L^{-1} are independent of flight condition, the solution for a desired modal response involves only the summation of the products of spanwise accelerometer signals and their corresponding constant matrix elements by an analog or digital device, here called a solver.

3. IDENTIFICATION OF MODAL RATE RESPONSE

Consider the block diagram shown in Figure 2. For modal acceleration $\ddot{x}$ and modal displacement x determined as above for any mode, this diagram represents the following filter equations from [7,9]:

$$-\frac{d}{dt}\hat{\dot{x}} = \hat{\ddot{x}} + K_1(x - \hat{x}) \tag{3}$$

$$\frac{d}{dt}\hat{\ddot{x}} = \ddot{x} + K_2(x - \hat{x}) \tag{4}$$

where the hatted quantities are estimated values, and K_1 and K_2 are constants. Writing the estimation error as

$$e = x - \hat{x}$$

and differentiating equation (3) with respect to time, there results

$$\frac{d^2}{dt^2}\hat{x} = -\frac{d}{dt}\hat{\ddot{x}} + K_1\dot{e} \qquad (5)$$

Substituting equation (4) into equation (5),

$$\frac{d^2}{dt^2}\hat{x} = \ddot{x} + K_2 e + K_1\dot{e} \qquad (6)$$

Since $\frac{d^2}{dt^2}\hat{x} - \ddot{x} = -\ddot{e}$, equation (6) becomes

$$\ddot{e} + K_1\dot{e} + K_2 e = 0 \qquad (7)$$

This expression represents the dynamics of the estimation error. The corresponding characteristic equation is

$$s^2 + K_1 s + K_2 = 0$$

The bandwidth and damping of the estimation process are determined by the choice of the constants K_1 and K_2.

Since the elements of the filter shown in Figure 2 are independent of flight condition, the estimation of modal rate response involves only the integration of the products of constants and the measured modal responses by an analog or digital device, here called a McKillip filter. Note that an improved estimate of the modal displacement x is also obtained due to the double integration of modal acceleration $\ddot{x}$ embodied in the filter. Also, note that no knowledge of the rotor or its flight condition is required in designing the filter.

4. FORM OF THE MODAL CONTROLLER

As discussed in the Introduction, the modal controller voltage output to the blade pitch actuator is proportional to modal acceleration, rate, and displacement:

$$V = -K_A\ddot{x} - K_R\dot{x} - K_P x$$

where K_A, K_R, and K_P are constants and therefore independent of flight condition.

For modal damping augmentation only,

$$V = -K_R\dot{x}$$

5. MODAL CONTROL BY INDIVIDUAL-BLADE-CONTROL (IBC)

The solver, McKillip filter, and controller described in Sections 2-4 are combined to form the IBC system for a given mode. The combined functions of the solver and the McKillip filter are here called the "observer". Some applications are described below, including experimental results obtained at MIT from a four-foot-diameter wind tunnel model rotor, using IBC.

Reference [3] describes the application of IBC to helicopter gust alleviation. The feedback blade pitch control was proportional to blade flapping acceleration and displacement, i.e.,

$$\Delta\theta = -K\left(\frac{\ddot{\beta}}{\Omega^2} + \beta\right)$$

A block diagram of the control system is shown in Figure 3. Note that each blade requires only two flatwise-oriented blade-mounted accelerometers.

Figure 4 shows the effect of increasing the open-loop gain K upon the IBC gust alleviation system performance. Note that the experimental reduction in gust-induced flapping response is in accordance with the theoretical closed-loop gain $1/(1+K)$.

The Lock number of the model blade was 3.0. For a full size rotor, the increase in damping due to the increase in Lock number results in the flapping at excitation frequency becoming the dominant response. Also, with increased blade damping it becomes possible to use higher feedback gain for the same stability level, and as a consequence the IBC system performance improves with increasing Lock number.

Following the successful alleviation of gust disturbances using the IBC system, Reference [3] showed the theoretical equivalence of blade flapping response due to atmospheric turbulence and that due to other low-frequency disturbances, e.g., helicopter pitch and roll attitude; therefore these disturbances can also be alleviated by the IBC system, as shown in [8], to provide helicopter attitude stabilization.

6. MODAL CONTROL USING A CONVENTIONAL SWASH PLATE

The preceding sections have demonstrated that the use of blade-mounted accelerometers as sensors makes possible the control of the flapping, flatwise bending, and lag modes of each blade individually. This control technique is applicable to helicopter rotor gust alleviation, attitude stabilization, vibration alleviation, and lag damping augmentation.

For rotors having three blades, any arbitrary pitch time history can be applied to each blade individually using the conventional swash plate. Rotors with more than three blades require individual actuators for each blade for some applications; for a rotor with four blades, other applications such as gust alleviation, attitude stabilization, vibration alleviation, and 1P lag damping augmentation can be achieved using a conventional swash plate, as shown in [8]. The summations of individual blade sensor signals required to obtain the swash plate collective and cyclic pitch components provide a filtering action such that only the desired harmonics 0P, 1P, 3P, 4P, and 5P remain after summation, i.e., no specific harmonic analysis is required.

Since all sensing is done in the blades, no transfer matrices from non-rotating to rotating system are required; therefore no updating of these matrices is required, and no non-linearity problems result from the linearization required to obtain the transfer matrices. Also, blade state measurements allow tighter vehicle control since rotor control can lead fuselage response: this lead should provide more effective gust alleviation and permit higher control authority without inducing rotor instabilities than would be possible without rotor state feedback [11].

7. BLADE FLAPPING RESPONSE FROM BLACK HAWK FLIGHT TESTS [12]

The objective of the flight measurements was to compare flapping estimated using the root and tip acceleration measurements with that predicted by a simple rigid-blade model, and with that measured by a root-mounted flapping transducer.

Time histories and frequency spectra of the two accelerometers for an 80 kt. level flight trim condition of the UH-60A helicopter, Figure 5, are shown in Figures 6 and 7. Multiple harmonics of rotor speed (4.3 Hz) are evident in the record, with 1P and 3P contributions being particularly strong. In order to estimate flapping for purposes of controlling flight dynamics, only the lower frequency responses at 0-1P are of interest. The analysis of [12] indicated significant 1P tip accelerometer response due to bending contributions to the local values of blade slope and blade acceleration, which together determine the tip accelerometer response. This was not the case for the root accelerometer.

The results suggested that blade 0-1P flapping estimation can be accomplished by using two inboard accelerometers to minimize the blade bending contribution to the accelerometer signals. Alternatively, the blade flapping and bending response can be determined by using four spanwise accelerometers and the methodology of Section 2 to solve for flapping and/or bending response.

The knowledge obtained from this test led to the use of two blade-root-mounted accelerometers in the Bell Model 412 wind tunnel tests described below.

8. BLADE LAG MOTION CONTROL FROM BELL MODEL 412 WIND TUNNEL TESTS [13]

Wind tunnel testing of the Model 412 rotor (Fig. 8) produced measurements of blade lag motion in inertial space for all four blades, using blade-root-mounted accelerometers. In the IBC system, Figure 9, these measurements are used to determine blade in-plane acceleration, estimated velocity, and displacement signals for each blade, and these signals are combined to generate inputs to the swash plate actuators; in the closed-loop system these inputs would provide helicopter blade in-plane damping augmentation.

Initial tests were open-loop, i.e., the output of the IBC system was not connected to the swash plate actuators. However, considerable insight into the closed-loop performance of the IBC system was obtained from the open-loop testing, as described below.

Recorded open-loop accelerometer signals were used as input to the IBC system of Figure 9 in the laboratory. The resulting cyclic control outputs are then compared with the desired closed-loop control displacements under the same disturbed test conditions.

The test disturbance was sinusoidal longitudinal (or lateral) displacement of the cyclic controls. This technique has been used successfully in the past [14]. As shown in [10], the closed-loop damping of blade lag motion is augmented by feeding back the lag rate to blade pitch.

Lag excitation tests were run at advance ratios 0 and .10 using swash plate excitation frequencies ω given by $\Omega-\omega = 0.9\,\omega_L$ to $1.10\,\omega_L$. A typical lag response time history and frequency spectrum from the tests is shown in Figures 10 and 11. The swash plate excitation frequency ω appears in the rotating systems as $(\Omega \pm \omega)$ where Ω is the rotor frequency. At lag resonance $\Omega - \omega = \omega_L$.

The analog data were then used to find the lag response characteristics of the Model 412 rotor to swashplate oscillations at discrete frequencies. Data records from 10 to 40 seconds were collected from the 8 accelerometers at each fixed excitation frequency to eliminate transient contamination of the estimates. Comparison of the lag sensor and the reconstructed lag signal from the observer in Figure 12 shows surprisingly good agreement, verifying the measurement of rotor states using blade-mounted accelerometers.

The final control system evaluation step concerned the investigation of the disturbance rejection capability of the control system design. This was achieved through comparison of the rotor pitch excitation used in the open-loop testing with the calculated rotor pitch to be fed back from the controller. Should these two signals cancel, one may infer that any other disturbances that would cause lag excitation could also be reduced through control of blade pitch through the swashplate. Figure 13 compares the pitch excitation measured on one of the blades with the pitch feedback signal from the controller. This feedback trace is inverted and offset in order to more closely compare the two signals. The controller output is the recombination of the feedback swash plate inputs in the rotating frame reference. The two curves can be seen to have similar shape, with the feedback signal slightly delayed due to the phase lag inherent in the filtering process.

9. BLADE FLAPPING MOTION CONTROL FROM BELL MODEL 412 WIND TUNNEL TESTS [15]

Wind tunnel testing of the Model 412 rotor (Fig. 8) in 1990 produced measurements of blade flapping motion in inertial space for all four blades, using root-mounted accelerometers. In the IBC system, Figure 14, these measurements are used to determine blade flapping acceleration, estimated velocity, and displacement signals for each blade, and these signals are combined to generate inputs to the swash plate actuators; in the closed-loop system these inputs would provide helicopter attitude stabilization and gust alleviation [8].

Initial tests were open-loop, i.e., the output of the IBC system was not connected to the swash plate actuators. However, considerable insight into the closed-loop performance of the IBC system was obtained from the open-loop testing, as described below.

Open-loop accelerometer signals recorded digitally were used as input to the IBC system of Figure 14 in the laboratory. The resulting cyclic control outputs are then compared with the desired closed-loop control displacements under the same disturbed test conditions. In-plane test data were presented in Section 8. The present section will present the flapping data in a similar manner.

The test disturbance was sinusoidal longitudinal (or lateral) displacement of the cyclic controls. This technique has been used successfully in the past [14]. As shown in Section 1, the closed-loop response of the rotor tip-path-plane to any disturbances is attenuated by the factor $1/(1+K)$ where $K = K_A = K_R = K_P$ is the gain of the IBC system. In the present open-loop case, the IBC system outputs were examined to see if, in the closed-loop case, they would provide the expected rotor response attenuation of $1/(1+K)$.

Flapping excitation tests were run at advance ratios 0, 0.1, and 0.2 using swash plate excitation frequencies $\omega = 0$ to 0.25Ω. Frequency spectra and a typical flapping accelerometer time history from the tests are shown in Fig. 15. The swash plate excitation frequency ω appears in the rotating system as $(\Omega \pm \omega)$ where Ω is the rotor frequency.

The first task concerned the performance of the rotor flap mode state estimator, as described in Sections 2 and 3. As the proposed IBC scheme involves feedback of flapping position, rate and acceleration, adequate performance of this portion of the controller would be indicated through comparison of similar measurements using sensors other than accelerometers. Since the 412 rotor is of hingeless design, flap position was recorded as scaled signals from a bending strain gauge located at 4.8% of the rotor radius. Figure 16 shows the time history from this strain gauge plotted above the flap displacement estimate from the observer. Differences in the two time histories can be explained through examination of the spectral content of the two signals, Figure 17, which differ primarily at frequencies above 1/rev. Such variation may be caused by the participation of higher out-of-plane modes in the gauge measurements, similar to the effects seen in the tip accelerometer measurements of [12]. Further examination of these data show that the flap sensor is nearly identical to another flap bending gauge located at 1.7% of rotor radius, which suggests that the sensor at 4.8% radius picks up all of the hub moment due to out-of-plane motion, and not just that from flapping (the first mode) alone. Based upon these arguments, the flap displacement estimator was deemed sufficiently accurate to warrant further investigation in a control system context.

The next step of the validation process was the reconstruction of a feedback signal to cancel the pitch excitation. This was done using a simple constant gain feedback, but through the full system of Figure 14, in which individual flap position, rate and acceleration estimates were generated for each blade, and then summed to provide swashplate command signals. These swashplate commands were then reconstructed to give the pitch signal that would be generated at the reference blade, and this is compared to the actual pitch excitation in Figure 18. The similarity of the two curves shows that such a system would indeed act to reduce unwanted disturbances that would generate excessive flapping response. Effects of alternate feedback strategies, and their influence on other modes (such as lag response) are discussed below.

If the simple feedback scheme of Figure 14 with $K_A = K_R = K_P$ is used, a root locus for the resulting closed-loop dynamics can be seen in Figure 19. This plot shows that the observer poles are not "controllable" through variations in the feedback gain K (as indicated by an exact pole-zero cancellation), a direct consequence of the use of the predictive nature of the acceleration measurement in the reconstruction of the flapping state estimates. As a result, feedback laws may be designed that assume full state feedback is present, without worry that the inclusion of an observer will deteriorate the predicted full-state feedback design dynamic properties. In addition, two complex dipoles are shown: the lower frequency, lightly damped pair represent the lag dynamics interaction with the flapping response, and the higher frequency, higher damping pair are the original flapping dynamics, along with a complex zero introduced through the selection of the ratio of the three gain constants K_P, K_R and K_A. Variations in the relative levels of these three constants would move this zero around the complex plane, such that increases in total loop gain would have the open-loop flap dynamics asymptotically approach these zeros. This behavior is very much like an implicit-model-following design, where feedback is structured to make the open-loop dynamics track a certain dynamic behavior.

As can be seen by the relatively small migration of the poles with feedback gain, this system (as modeled here) will be robust to gain variations with flight condition, and will lessen the influence of the lag dynamics on the flap motion as a result of the pole-zero cancellation present for this mode. The disturbance response, due to the close proximity of the zeros near the flapping mode poles, will have quite similar dynamics to the open-loop behavior, but at a significantly lower amplitude. This result is further confirmed by examining the flapping response of this system to a step aerodynamic disturbance at a moderate feedback gain level, shown in Figure 20. It can be seen the response diminishes the oscillatory behavior from the lag coupling, while reducing the net excursion level by $1/(1+K)$.

10. HELICOPTER VIBRATION ALLEVIATION [5, 8]

In the IBC bending control system, Figure 21, measurements of blade flatwise motion in inertial space, using four blade-mounted accelerometers, are used to determine blade bending acceleration, estimated velocity, and displacement signals for each blade, (see Section 2), and these signals are combined to generate inputs to the swash plate actuators; in the closed-loop system these inputs would provide helicopter blade bending attenuation, with resulting vibration alleviation. Since the first blade flatwise bending mode is a major contributor to rotor vibration, alteration of the dynamics of this mode can substantially reduce helicopter vibration, as shown in Figure 22, taken from [16].

Further discussion of measurement of blade flatwise motion is contained in [17]. The reference presents comparisons of blade first mode bending displacements as estimated by blade-mounted accelerometers and blade-mounted strain gauges, as shown in Figure 23.

11. SUMMARY AND CONCLUDING REMARKS

During the period 1977 - 1985 extensive theoretical and experimental research was conducted at MIT on helicopter Individual-Blade-Control (IBC). The experimental portion of this research consisted of wind tunnel testing of small models. The next phase of the research was conducted under a cooperative agreement with Ames Research Center, NASA, and involved full-size flight and wind tunnel testing of a Sikorsky Black Hawk and a Bell Model 412 respectively. These open-loop tests occurred in 1987 and 1990. Unfortunately, due to external constraints, both tests were small adjuncts to much larger unrelated tests. To this date no closed-loop tests have been conducted. However, considerable new knowledge of IBC system components was acquired.

The unique characteristics of IBC can be summarized as follows:

1. Individual control of the lift on each blade, or a portion thereof, by such means as conventional blade pitch, partial-span flap or flaps, local or distributed circulation control, or "smart structures".

2. An inner feedback control loop around each blade in the rotating system. Specialized complete-vehicle functions can be achieved by outer loops, which can operate at high gain since blade stability is ensured by the inner loop.

3. Item (2) can only be achieved by the use of individual sensors on each blade, such as accelerometers.

Accelerometers offer many advantages as sensors in the rotating system. Their use is well-established in the suppression of high-frequency flutter and vibration in fixed wing aircraft. The accelerometer signal can be integrated once and twice to obtain high-fidelity rate and displacement estimates.

4. Control in the time-domain: this approach eliminates the need for harmonic analysis or filtering found in HHC systems, with their corresponding lags and inability to follow rapid transients such as those found in helicopter maneuvering flight. Also, control of the stability of various blade modes becomes possible.

The future of IBC can be summarized as follows:

1. Helicopter blades will utilize blade-mounted sensors, probably accelerometers, as Individual-Blade-Sensors (IBS). This will be true for both swash-plate controlled and Individual-Blade-Control rotors.

2. Initial IBC rotors will probably embody extensible pitch links supplemental to the conventional swash plate.

3. Later IBC rotors will utilize local blade lift changes resulting from partial span flaps, circulation control, or deformable structures.

4. It is possible that the many advantages of IBC will lead to a return to three-bladed rotors having IBS and a conventional swash plate for small and medium helicopters, and coaxial three-bladed rotors, each with its own swash plate, for large helicopters.

REFERENCES

1. Kretz, M., "Research in Multicyclic and Active Control of Rotary Wings," Vertica, 1, 95-105, 1976.

2. Ham, N.D., "A Simple System for Helicopter Individual-Blade-Control Using Modal Decomposition", Vertica, 4, 23-28, 1980.

3. Ham, N.D. and McKillip, R.M., Jr., "A Simple System for Helicopter Individual-Blade-Control and Its Application to Gust Alleviation", Proc. Thirty-Sixth AHS Annual National Forum, Washington, D.C., May 1980.

4. Ham, N.D. and Quackenbush, T.R., "A Simple System for Helicopter Individual-Blade-Control and Its Application to Stall-Induced Vibration Alleviation", Proc. AHS National Specialists' Meeting on Helicopter Vibration, Hartford, CT, November 1981.

5. Ham, N.D., "Helicopter Individual-Blade-Control and Its Applications", Proc. Thirty-Ninth AHS Annual National Forum, St. Louis, MO, May 1983.

6. Ham, N.D., Behal, Brigitte L. and McKillip, R.M., Jr., "Helicopter Rotor Lag Damping Augmentation Through Individual-Blade-Control", Vertica, 7, 361-371, 1983.

7. McKillip, R.M., Jr., "Periodic Control of the Individual-Blade-Control Helicopter Rotor", Vertica, 9, 199-224, 1985.

8. Ham, N.D., "Helicopter Gust Alleviation, Attitude Stabilization, and Vibration Alleviation Using Individual-Blade-Control Through a Conventional Swash Plate", Proc. Forty-First AHS Annual National Forum, Fort Worth, Texas, May 1985.

9. McKillip, R.M., Jr., "Kinematic Observers for Rotor Vibration Control," Proc. Forty-Second AHS Annual National Forum", June 1986.

10. Ham, N.D., "Helicopter Individual-Blade-Control Research at MIT 1977-1985," Vertica, 11, 109-122, 1987.

11. DuVal, R.W., "Use of Multiblade Sensors for On-Line Rotor Tip-Path-Plane Estimation," IAHS 25, 4, October 1980.

12. Ham, N. D.; Balough, D.L.; and Talbot, P.D., "The Measurement and Control of Helicopter Blade Modal Response Using Blade-Mounted Accelerometers", Proc. Thirteenth European Rotorcraft Forum, September, 1987.

13. Ham, N.D., and McKillip, R.M. Jr., "Research on Measurement and Control of Helicopter Rotor Response Using Blade-Mounted Accelerometers 1990-91," Proc. 17th European Rotorcraft Forum, Berlin, Germany, September 1991.

14. Kaufman, L., and Peress, K., "A Review of Methods for Predicting Helicopter Longitudinal Response," Journal of The Aeronautical Sciences, March, 1956.

15. Ham, N.D., and McKillip, R.M. Jr., "Research on Measurement and Control of Helicopter Rotor Response Using Blade-Mounted Accelerometers 1991-92," Proc. 18th European Rotorcraft Forum, Avignon, France, September 1992.

16. Leone, P.F., "A Method for Reducing Helicopter Vibration," IAHS 2, 3, July 1957.

17. Ham, N.D., and McKillip, R.M., Jr., and Balough, D.L., "Research on Measurement and Control of Helicopter Rotor Response Using Blade-Mounted Accelerometers 1992-93," Proc. Nineteenth European Rotorcraft Forum, Como, Italy, September 1993.

Acknowledgments

The author wishes to acknowledge the major contributions of Dr. Robert M. McKillip, Jr. to the research described in this paper, a product of our collaboration from 1978 to the present.

The author also wishes to acknowledge Ames Research Center, NASA, for financial support under Cooperative Agreements NCC 2-366 and NCC 2-447, and for the provision of wind tunnel and flight test data.

The author is grateful to Carolyn Fialkowski for her expert and patient typing of the paper.

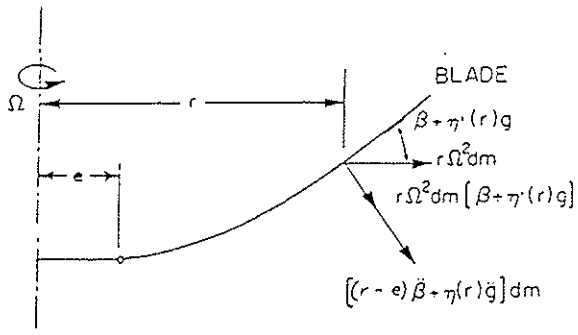

Figure 1. Blade Flatwise Inertia Forces

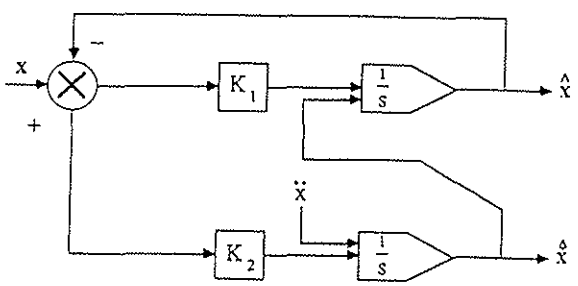

Figure 2. Block Diagram of McKillip Filter

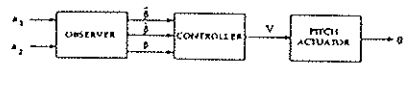

Figure 3. Block Diagram of Flapping IBC System

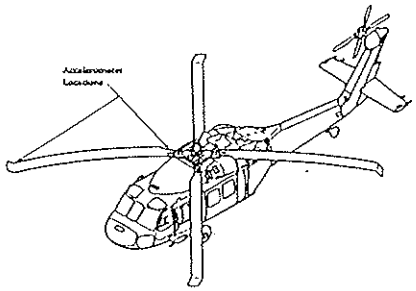

Figure 5 The Sikorsky Black Hawk Helicopter

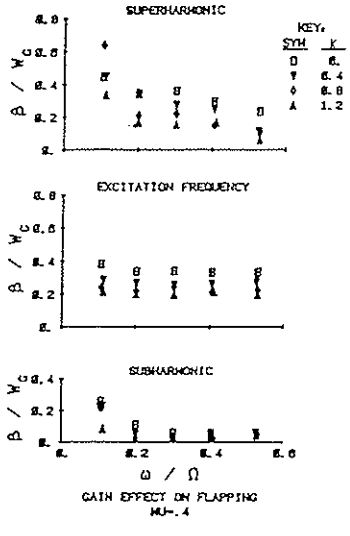

Figure 4. Effect of Feedback Gain on Flapping Response to Gust (μ = 0.4)

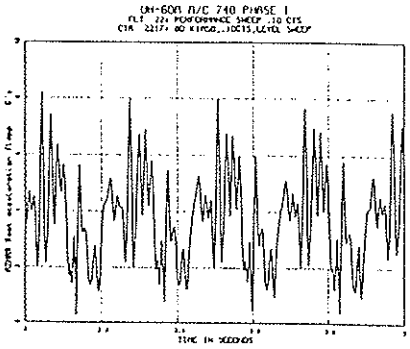

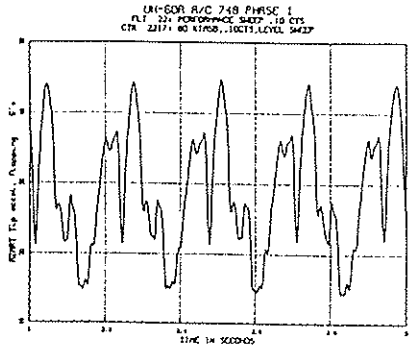

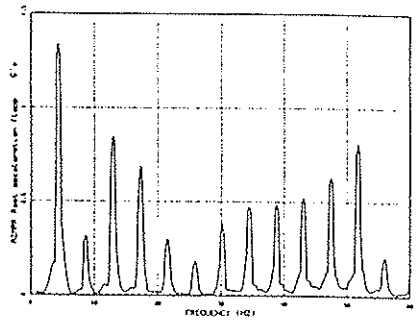

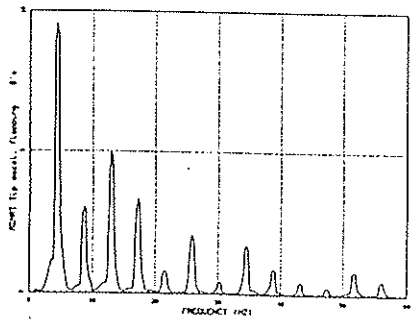

Figure 6. Root Accelerometer Time History and Frequency Spectrum

Figure 7 The Accelerometer Time History and Frequency Spectrum

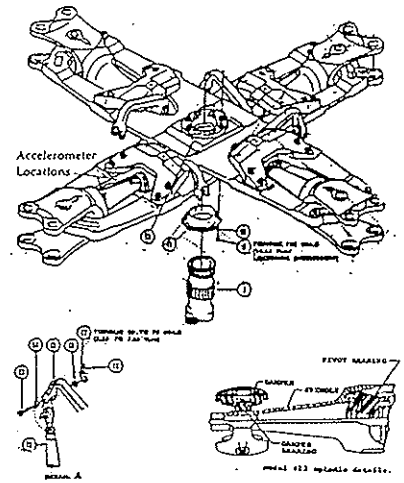

Figure 8. Model 412 Main Rotor Hub

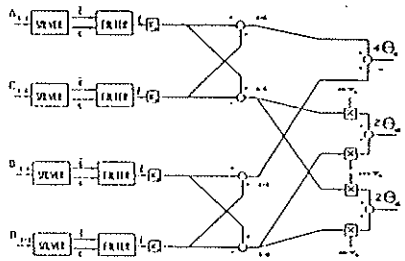

Figure 9. Schematic of Blade Lag Control System Using the Conventional Swash Plate: Four-Bladed Rotor.

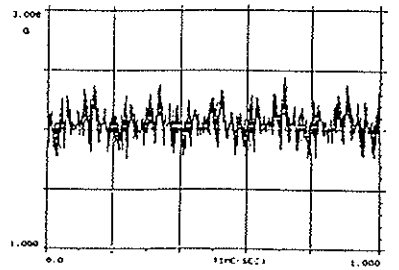

Figure 10. Typical lag Accelerometer Time History: μ = 0.1, ω = 1.8 Hz.

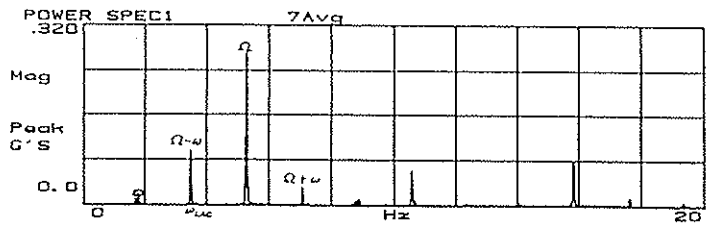

Figure 11. Typical Lag Accelerometer Frequency Spectrum; μ = 0.2, ω = 1.8 Hz.

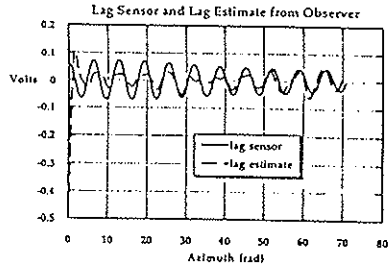

Figure 12 Comparison of Blade Lag Angle as Measured by Potentiometer and by Accelerometers

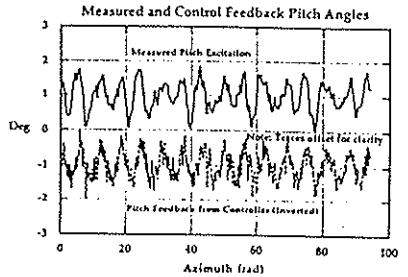

Figure 13 Comparison of Blade Pitch Excitation and IBC Pitch Feedback

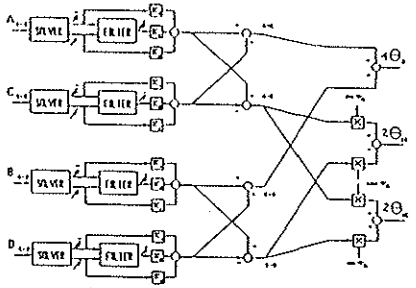

Figure 14. Schematic of Flapping Control System Using the Swash Plate: Four-Bladed Rotor

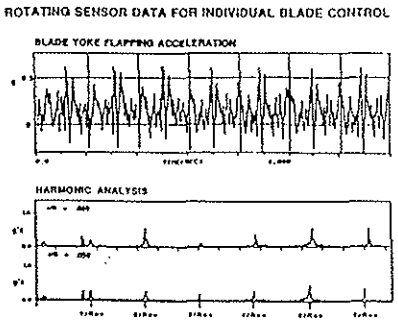

Figure 15. Bell 412 blade yoke acceleration data. Rotor at 316 RPM, 4° collective, -8° shaft angle, 0.2 advance ratio, and 0.8 Hz, swashplate excitation at ±0.5°

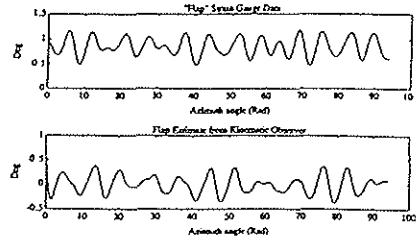

Figure 16. Comparison of Flap Gauge Signal with Flap Estimate, Hover.

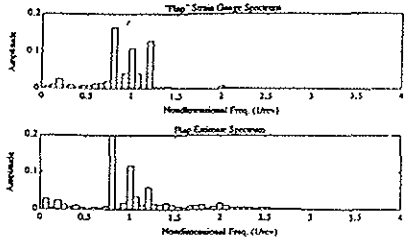

Figure 17. Comparison of Flap Gauge and Flap Estimate Spectra.

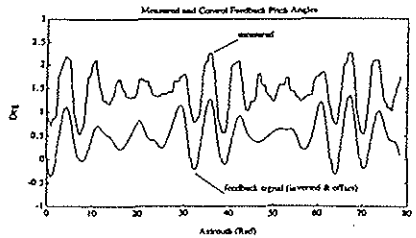

Figure 18. Measured and Control System Feedback (Inverted) Pitch Angles.

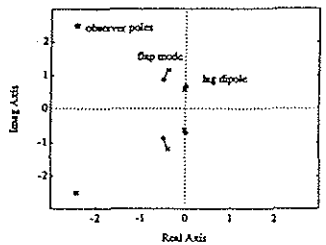

Figure 19. Root locus for flap mode feedback: K_A=K_B=K_F=K.

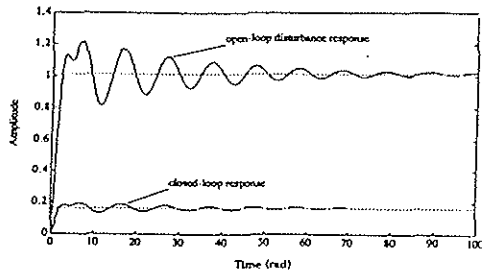

Figure 20. Open- and closed-loop disturbance step response, flap mode feedback: K_A=K_B=K_F=K.

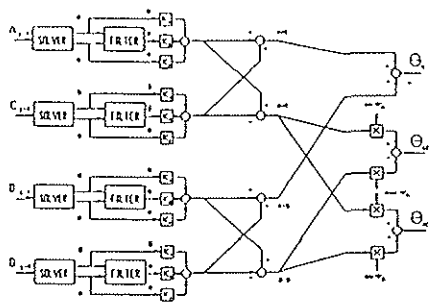

Figure 21. Schematic of Bending Control System Using the Swash Plate: Four-Bladed Rotor

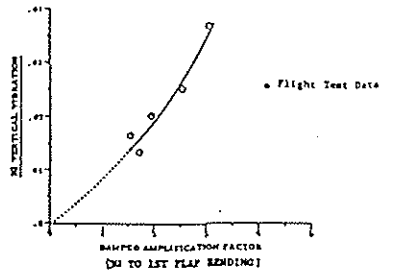

Figure 22. Effect of Blade Bending Amplification Factor on Maximum Cockpit Vibration Level

Spectral Magnitude Comparison: Bending Mode Reconstruction From Blade Sensor Signals

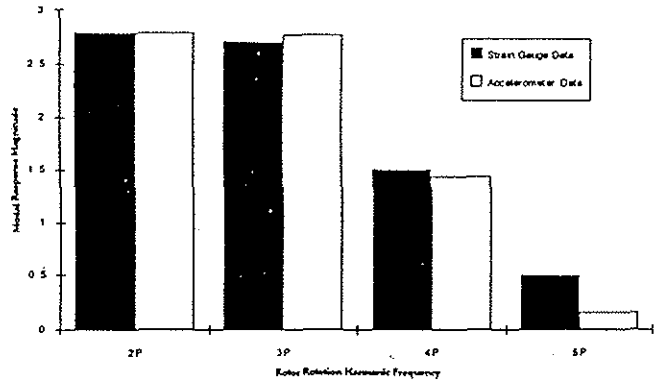

Figure 23. Comparison of Bending Response Spectral Components: Strain Gauge-Based Estimates / Accelerometer-Based Estimates